Available online at www.sciencedirect.com
SCIENCE DIRECT®
Journal of Power Sources 133 (2004) 32–38
JOURNAL OF POWER SOURCES
www.elsevier.com/locate/jpowsour

In situ electrochemical atomic force microscopy of lead electrodes in sulfuric acid solution with or without lignin during anodic oxidation and cathodic reduction

N. Hirai [a,*], D. Tabayashi [a], M. Shiota [b], T. Tanaka [a]

[a] *Department of Materials Science and Processing, Graduate School of Engineering, Osaka University, Yamadaoka 2-1, Suita, Osaka 565-0871, Japan*
[b] *Yuasa Corporation, 2-3-21 Kosobe-cho, Takatsuki, Osaka 569-1115, Japan*

Received 11 August 2003; accepted 8 December 2003

Abstract

The surface morphologies of lead sheets in sulfuric acid solution, with or without lignin, under temperature control during anodic oxidation and cathodic reduction are investigated by using in situ electrochemical atomic force microscopy combined with cyclic voltammetry. Whether lignosulfonate (lignin) is added or not, it is found at −20 °C that the precipitation of lead sulfate crystals occurs immediately after supersaturation of dissolved Pb^{2+} ions at the anodic oxidation peak on the cyclic voltammogram. It is also observed that the density of lead sulfate crystals formed on the lead electrode after anodic oxidation decreases and the crystal size becomes larger when lignin is added. Furthermore, the addition of lignin delays dissolution of lead sulfate crystals during cathodic reduction at room temperature (RT).

Keywords: Electrochemical atomic force microscopy (EC-AFM); Lead−acid battery; Negative electrode; Expander; Lignosulfonate (lignin); Cyclic voltammetry (CV)

1. Introduction

Lead–acid batteries have been widely used as power sources of automobiles and uninterruptible power supplies. More recent applications include power supplies for hybrid electric vehicles and load-leveling systems. It is important to understand in detail the reactions on the electrodes of the battery, and the effect of additives on these reactions during charging or discharging, in order to construct an improved battery with suitable performance for each application. Lignosulfonate (lignin) is commonly used as an additive for the negative electrode (paste). It is known that lignin influences the performance of the lead–acid battery, as well as the characteristics of the negative paste [1]. For example, lignin increases the discharge capacity at low temperature and improves cycle-life [2], but lowers the charge acceptance [3]. Nevertheless, the detailed mechanism of the effect of lignin has still to be elucidated.

Electrochemical atomic force microscopy (EC-AFM) is a powerful investigative tool—it can be used for the in situ examination of electrode surfaces in electrolytes. Not only atomic or molecular arrangements of single crystals on the electrode, but also the morphology of the electrode itself at the micron scale, can be observed by means of EC-AFM. Previous studies [4–10] have used EC-AFM to monitor morphological changes on a Pb or PbO_2 surface in sulfuric acid solution. These observations provide considerable information on electrochemical reactions on electrodes in lead–acid batteries. The first EC-AFM observation of the effect of lignin on the electrochemical reaction at a lead electrode was performed by Ban et al. [8]. In that work, lead sheets, whose surface oxide layers were chemically etched, were examined in sulfuric acid solution, with or without lignin, at room temperature (RT), both before and after anodic oxidation. In more recent work, it has been shown that the oxide layer on the lead surface reacts with the lignin [11,12], and that this reaction plays an important role in the electrochemical characteristics of lead electrodes [12].

In this study, the behaviour of lead electrodes in sulfuric acid solution with lignin is investigated by means of EC-AFM and under the following experimental conditions.

(i) The electrodes are lead sheets with the surface oxide layers not removed.
(ii) Continuous EC-AFM combined with cyclic voltammetry (CV) is performed in order to observe the electrode reaction dynamically in the presence of lignin.

* Corresponding author. Tel.: +81-6-6879-7468; fax: +81-6-6879-7468.
E-mail address: nhirai@mat.eng.osaka-u.ac.jp (N. Hirai).

0378-7753/$ – see front matter © 2004 Elsevier B.V. All rights reserved.
doi:10.1016/j.jpowsour.2003.12.020

(iii) The electrodes are examined during anodic oxidation at −20 °C.
(iv) The electrodes are examined during cathodic reduction at RT.

2. Experimental

2.1. EC-AFM

A schematic illustration of the EC-AFM equipment is given in Fig. 1. The EC-AFM is composed of an atomic force microscope (Pico SPM, Molecular Imaging Co.), a control unit (Pico Scan 2100, Molecular Imaging Co.), an electrochemical cell, and some electrochemical devices. The electrochemical cell comprised the lead working electrode with a PbO_2 counter electrode and a $Hg|Hg_2SO_4$ reference electrode. All potentials are reported with respect to the reference electrode. Cyclic voltammetry was performed with a potentio/galvanostat (Model HZ-3000, Hokuto Denko Co). The sample temperature (−20 °C or RT) was regulated by a Peltier device with a control unit (Model 321, Lake Shore Co). All experiments were conducted in a chamber that was filled with argon gas to prevent oxidation of the electrode.

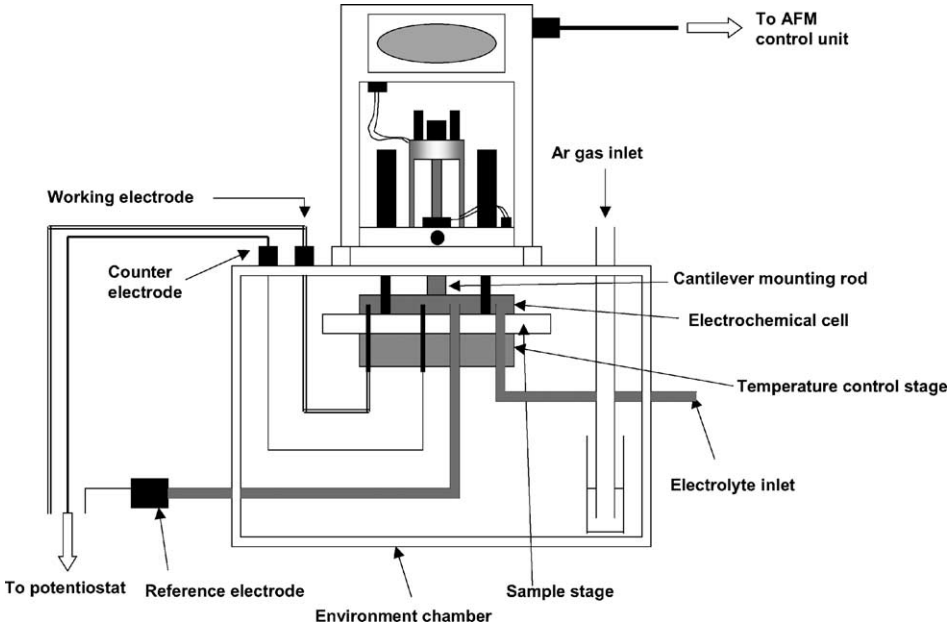

Fig. 1. Schematic illustration of EC-AFM equipment.

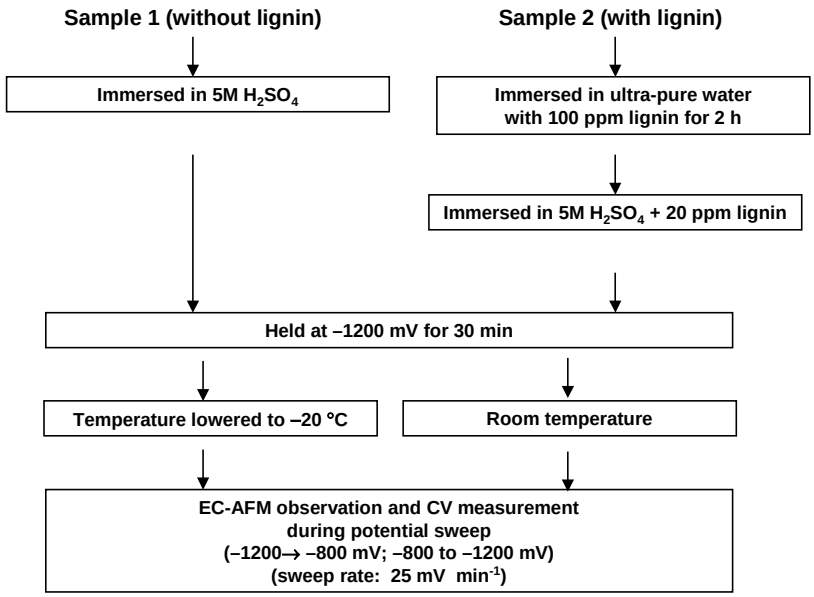

Fig. 2. Experimental procedure for EC-AFM and CV investigations.

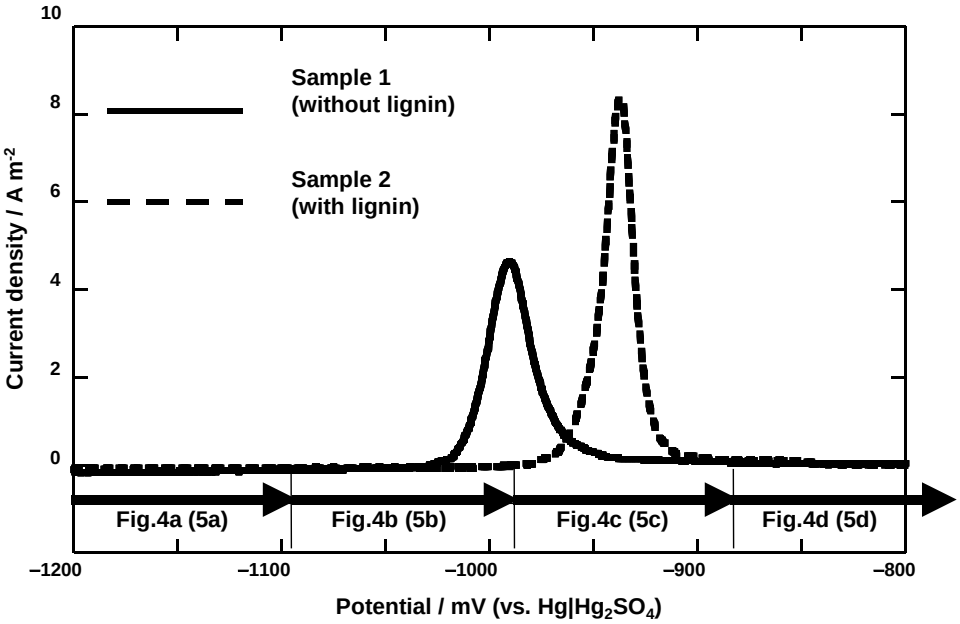

Fig. 3. Cyclic voltammograms for lead electrodes at −20 °C in 5M H_2SO_4 (solid line) and in 5 M H_2SO_4 with 20 ppm lignin (broken line) during positive-going scan at 25 mV min^{-1}. Sequence of EC-AFM images (Figs. 4 and 5) is indicated.

2.2. Experimental preparation of electrodes for EC-AFM and CV

Lead electrodes (samples 1 and 2) were prepared from pure-lead sheets (99.99%, Niraco Co). Before EC-AFM or CV, sample 1 was immersed in 5 M sulfuric acid solution without lignin. On the other hand, sample 2 was immersed for 2 h in ultra-pure water with 100 ppm lignin in order to form a film that contained lead and lignin on the electrode surface [12]. The chosen lignin was 'Vanillex N' (Nippon Paper Industries Co.). The electrolyte was then replaced by 5 M sulfuric acid solution that contained 20 ppm lignin. Immediately after immersion (sample 1 in 5 M sulfuric acid; sample 2 in 5 M sulfuric acid with 20 ppm lignin), a potential

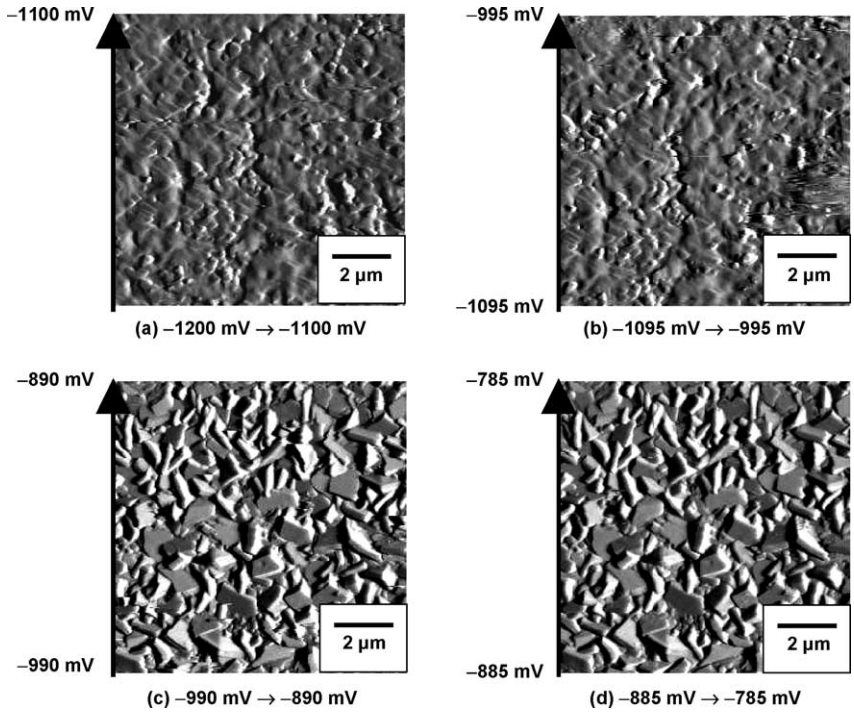

Fig. 4. Continuous in situ EC-AFM images of lead electrode surface in 5 M H_2SO_4 without lignin (sample 1) at −20 °C during voltammetric scan shown in Fig. 3. Direction of slow scan of EC-AFM images indicated by arrows.

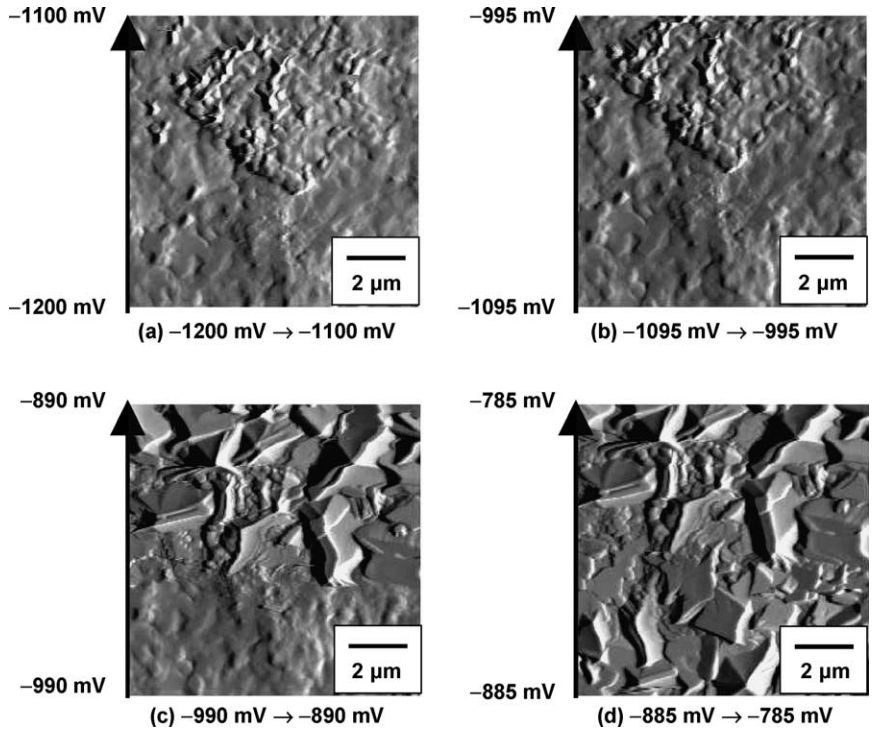

Fig. 5. Continuous in situ EC-AFM images of lead electrode surface in 5 M H_2SO_4 with 20 ppm lignin (sample 2) at −20 °C during voltammetric scan shown in Fig. 3. Direction of slow scan of EC-AFM images indicated by arrows.

of −1200 mV was applied for 30 min to reduce the lead oxide and/or lead sulfate on the lead surface. After this reduction, the temperature was lowered to −20 °C for EC-AFM or CV investigation. An outline of the experimental procedure is presented in Fig. 2.

3. Results and discussion

3.1. CV during anodic oxidation at −20 °C

Cyclic voltammograms for sample 1 (in sulfuric acid solution without lignin; solid line) and sample 2 (in sulfuric acid solution with 20 ppm lignin; broken line) at −20 °C during a positive-going scan from −1200 to −800 mV at 25 mV min^{-1} are shown in Fig. 3. The anodic current corresponds to the conversion of lead to lead sulfate, i.e., $Pb + SO_4^{2-} \rightarrow PbSO_4 + 2e^-$. The capacity of sample 2 is about 160% larger than that of sample 1. This result supports the fact that the discharge capacity of lead–acid batteries increases on the addition of lignin.

3.2. EC-AFM during anodic oxidation at −20 °C

Before CV, the immersed electrodes were observed by EC-AFM in order to confirm that no lead sulfate crystals were present on the surfaces. Then, the surface morphologies of the electrodes during a positive-going sweep from −1200 to −785 mV at 25 mV min^{-1} were investigated by

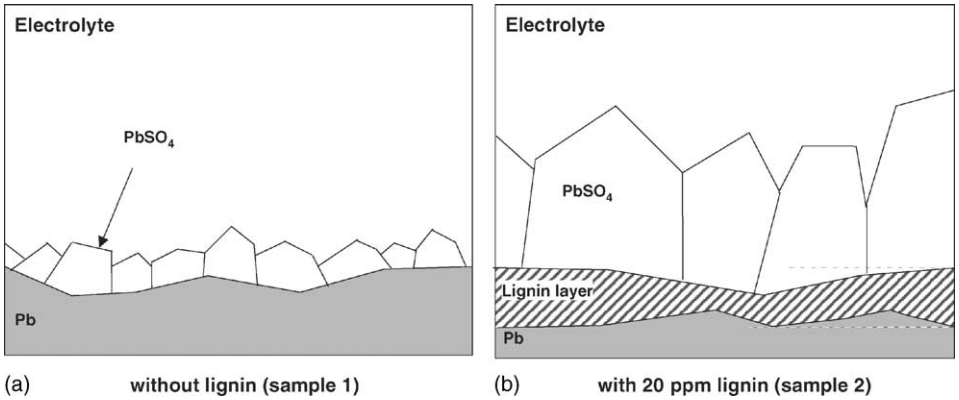

Fig. 6. Schematic illustration of cross-section near electrode surface.

using in situ EC-AFM. Because the capturing rate was about 4 min per one AFM image, about four in situ EC-AFM images (10 μm × 10 μm) could be captured during one anodic sweep, as shown in Fig. 3.

The in situ EC-AFM images (10 μm × 10 μm) for sample 1(without lignin) and sample 2 (with 20 ppm lignin) are presented in Figs. 4 and 5, respectively. Few morphological changes are observed for either sample until the anodic current reaches the maximum of the peak in the respective cyclic voltammogram. Thereafter, the precipitation of many lead sulfate crystals takes place. In a solution without lignin at RT, it has been visually confirmed [5] that lead dissolves during the anodic oxidation ($Pb \rightarrow Pb^{2+} + 2e^{-}$), followed by the precipitation of $PbSO_4$ crystals immediately after supersaturation of dissolved Pb^{2+} ions ($Pb^{2+} + SO_4^{2-} \rightarrow PbSO_4$). These processes constitute a 'solution–precipitation mechanism' [13]. The results given in Figs. 3–5 show that $PbSO_4$ is formed at −20 °C mainly by the this mechanism, irrespective of the presence of lignin.

It is also found (Figs. 4 and 5) that the density of the $PbSO_4$ crystals formed on the lead electrode after anodic oxidation decreases and the crystal size becomes larger when lignin is added to the solution. A schematic illustration of the cross-section near the electrode surface of samples 1 and 2 is shown in Fig. 6(a) and (b), respectively. The larger crystal size in the presence of lignin agrees with the experimental results that the anodic capacity of the cyclic voltammogram becomes larger when lignin is added to the solution, as already shown in Fig. 3. It is concluded that the increase in the size of the crystals in the presence of lignin is due to a decrease in the density of the nuclei. The density of three-dimensional critical nuclei, N^*, can be expressed by the following equation;

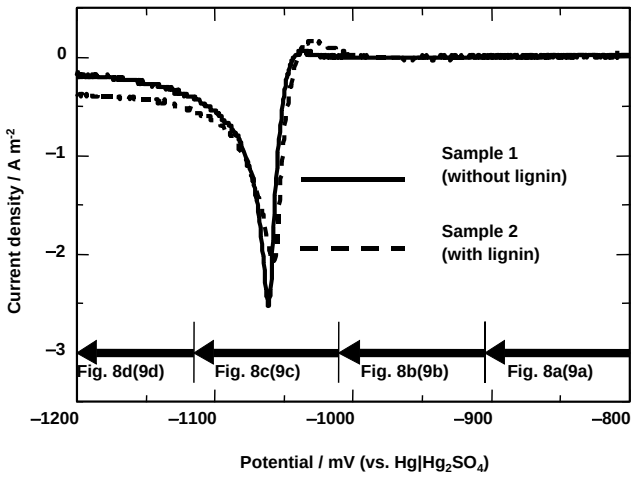

Fig. 7. Cyclic voltammograms for lead electrodes at RT in 5 M H_2SO_4 (solid line) and in 5 M H_2SO_4 with 20 ppm lignin (broken line) during negative-going scan at 25 mV min^{-1}.

$$N^* \propto \exp\left(\frac{-\Delta G^*}{kT}\right) = \exp\left[\frac{-\pi(2\gamma_{PbSO_4} + \gamma_I - \gamma_S)^3}{3k^3T^3n_0^2(\log(1+\sigma))^2}\right] \quad (1)$$

where, ΔG^* is the Gibbs free energy of a critical nucleus; γ_{PbSO_4} the surface tension of lead sulfate; γ_I the interfacial tension between lead sulfate and the substrate; γ_S the sur-

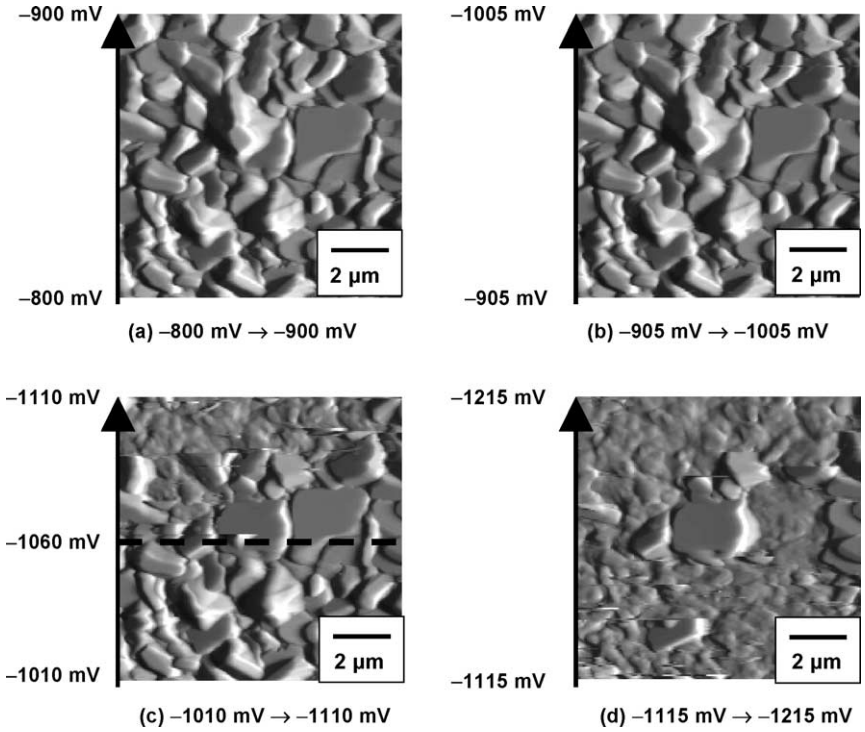

Fig. 8. Continuous in situ EC-AFM images of lead electrode surface in 5 M H_2SO_4 without lignin (sample 1) at RT during voltammetric scan shown in Fig. 7. Direction of slow scan of EC-AFM images indicated by arrows.

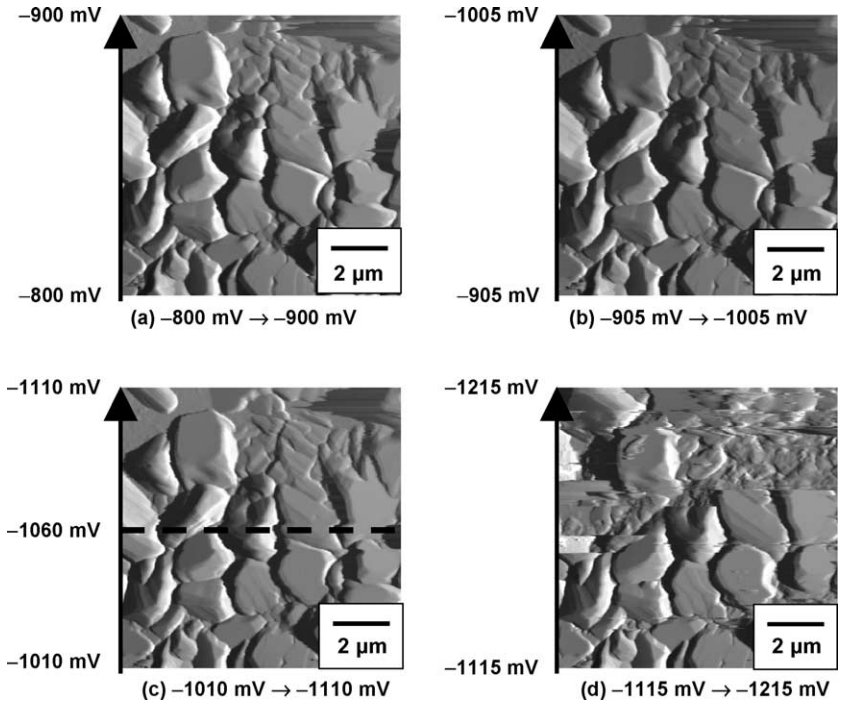

Fig. 9. Continuous in situ EC-AFM images of lead electrode surface in 5 M H_2SO_4 with 20 ppm lignin (sample 2) at RT during voltammetric scan shown in Fig. 7. Direction of slow scan of EC-AFM images indicated by arrows.

face tension of the substrate; n_0 the atomic density of lead atoms in lead sulfate; and σ is the supersaturation. It is considered that the γ_S of sample 2 is much smaller than that of sample 1 because the surface of the former is covered by lignin. Therefore, N^* of sample 2 is considered to be much smaller than that of sample 1. This agrees empirically with the EC-AFM images.

3.3. EC-AFM and CV during cathodic reduction at RT

Cyclic voltammograms for sample 1 (in sulfuric acid solution without lignin; solid line) and sample 2 (in sulfuric acid solution with 20 ppm lignin; broken line) at RT during a negative-going scan from −800 to −1200 mV at a sweep rate of 25 mV min^{-1} are shown in Fig. 7. The cathodic current corresponds to the conversion of lead sulfate to lead, i.e., $PbSO_4 + 2e^- \rightarrow Pb + SO_4^{2-}$. The corresponding in situ EC-AFM images (10 μm × 10 μm) for sample 1 (without lignin) and sample 2 (with 20 ppm lignin) are presented in Figs. 8 and 9, respectively. The lead sulfate crystals have almost vanished in Fig. 8(d), but are virtually unaffected in Fig. 9(d). These EC-AFM images indicate that the decay of lead sulfate is much slower in the solution with lignin. This delay in the decay is consistent with the fact that lignin lowers the charge acceptance of the electrode.

4. Conclusions

The electrochemical behaviour of lead electrodes in 5 M sulfuric acid solution with 20 ppm lignin or without lignin during anodic oxidation at −20 °C and during cathodic reduction at RT has been investigated by in situ EC-AFM and CV. The following conclusions have been reached.

1. Whether lignin is added or not, the precipitation of lead sulfate crystals occurs immediately after supersaturation of dissolved Pb^{2+} ions at the anodic oxidation peak of the cyclic voltammogram, even at −20 °C.
2. The density of lead sulfate crystals formed on the lead electrode after anodic oxidation decreases, and the crystal size becomes larger, when the lignin is added.
3. The addition of lignin delays dissolution of lead sulfate crystals during cathodic reduction at RT.

Acknowledgements

The authors are grateful to Prof. Shigeta Hara of Osaka University and Ikumi Ban of Yuasa Corporation for detailed discussion of the work. The study was partly supported by the 2001–2003 Industrial Technology Research Grant Program (ID number, 01B60015C) of the New Energy and Industrial Technology Development Organization (NEDO) of Japan.

References

[1] D.A.J. Rand, D.P. Boden, C.S. Lakshmi, R.F. Nelson, R.D. Prengaman, J. Power Sources 107 (2002) 280–300.
[2] A.C. Zachlin, J. Electrochem. Soc. 98 (1951) 325–333.

[3] P. Ekdunge, K.V. Rybalka, D. Simonsson, Electrochim. Acta 32 (1987) 659–667.
[4] Y. Yamaguchi, M. Shiota, Y. Nakayama, N. Hirai, S. Hara, J. Power Sources 85 (2000) 22–28.
[5] Y. Yamaguchi, M. Shiota, Y. Nakayama, N. Hirai, S. Hara, J. Power Sources 93 (2001) 104–112.
[6] M. Shiota, Y. Yamaguchi, Y. Nakayama, K. Adachi, S. Taniguchi, N. Hirai, S. Hara, J. Power Sources 95 (2001) 203–208.
[7] Y. Yamaguchi, M. Shiota, Y. Nakayama, M. Hosokawa, N. Hirai, S. Hara, J. Power Sources 102 (2001) 156–162.
[8] I. Ban, Y. Yamaguchi, Y. Nakayama, N. Hirai, S. Hara, J. Power Sources 107 (2002) 167–172.
[9] M. Shiota, Y. Yamaguchi, Y. Nakayama, N. Hirai, S. Hara, J. Power Sources 113 (2003) 277–280.
[10] N. Hirai, K. Takeda, S. Hara, M. Shiota, Y. Yamaguchi, Y. Nakayama, J. Power Sources 113 (2003) 329–334.
[11] B.O. Myrvold, J. Power Sources 117 (2003) 187–202.
[12] K. Saito, N. Hirai, M. Shiota, Y. Yamaguchi, Y. Nakayama, S. Hara, J. Power Sources 124 (2003) 266–270.
[13] G. Archdale, J.A. Harrison, J. Electroanal. Chem. 39 (1972) 357–366.